JACS
JOURNAL OF THE AMERICAN CHEMICAL SOCIETY

COMMUNICATION

pubs.acs.org/JACS

Dynamic Cylindrical Assembly of Triblock Copolymers by a Hierarchical Process of Covalent and Supramolecular Interactions

Zhou Li,[†] Jun Ma,[†] Nam S. Lee,[†,‡] and Karen L. Wooley*[,†,‡]

[†]Department of Chemistry, Washington University in St. Louis, St. Louis, Missouri 63130, United States

[‡]Department of Chemistry and Department of Chemical Engineering, Texas A&M University, College Station, Texas 77842, United States

Supporting Information

ABSTRACT: We have developed a hierarchical process that combines linear triblock copolymers into concentric globular subunits through strong chemical bonds and is followed by their supramolecular assembly *via* weak noncovalent interactions to afford one-dimensionally assembled, dynamic cylindrical nanostructures. The molecular brush architecture forces triblock copolymers to adopt intramolecular interactions within confined frameworks and then drives their intermolecular interactions in the mixtures of organic solvent and water. In contrast, the triblock copolymers, when not preconnected into the molecular brush architectures, organize only into globular assemblies.

Nature has evolved a complicated process to create sophisticated functional materials through hierarchical self-assembly of simple nanoscale motifs.[1−3] With the broader development of nanotechnologies, much effort has been made to understand and mimic this process to construct artificial nanostructures from synthetic molecules in the laboratory. Molecules with selective physical or chemical interactions are designed to drive the assembly processes, and various nanostructures with different functions have been obtained by tuning the properties of the synthetic molecules.[4−17] Among those molecules, block copolymers are of great interest.[4,5,8,13,16,18] However, the complexities of nanostructures derived from block copolymers remain lower than those from Nature, possibly because their structures are usually simpler than those originating from biomolecules. Herein, we demonstrate that dynamic hierarchical cylindrical assembly of triblock copolymers is achieved by stepwise application of covalent bonds and supramolecular interactions. Linear ABC triblock copolymers were initially prepared and then linked together by selective reaction through a single chain end site on each polymer chain, to establish a covalent molecular brush architecture. This process was followed by multimolecular supramolecular assembly in water to afford dynamic nanocylindrical assemblies, whereas the linear triblock copolymer precursor was incapable of producing such a unique morphology.

Molecular brushes are nonlinear macromolecules, in which many polymeric side chains are distributed along a backbone.[19,20] Generally, there are three strategies to synthesize molecular brushes: "grafting-from" (polymerization of side chains from initiating groups along a backbone),[21−23] "grafting-onto" (addition of previously synthesized side chains to a backbone),[24] and "grafting-through" (polymerization of the chain end groups of previously synthesized macromonomers).[25−28] Although molecular brushes with long backbones have been synthesized by "grafting-from" and "grafting-onto" approaches, it has been difficult to control the side chain grafting density and ensure control over the final compositions by these two strategies.[19,20] The "grafting-through" strategy is favored for good control over both grafting density and side chain structures.

The "grafting-through" strategy is a highly efficient process to synthesize block copolymer-based molecular brushes, for which we have developed a special case that combines four different polymer compositions, organized topologically within the macromolecular framework, by two controlled polymerization techniques: Reversible addition−fragmentation chain transfer (RAFT) polymerization and ring-opening metathesis polymerization (ROMP).[25,28−30] A molecular brush with polystyrene, poly(methyl acrylate), and poly(acrylic acid) triblock side chains grafted along a polynorbornene backbone was synthesized in three steps, including RAFT, ROMP, and deprotection (Figure 1A).

In the first step, the triblock macromonomer, α-norbornenyl polystyrene-*b*-poly(methyl acrylate)-*b*-poly(*tert*-butyl acrylate) (NB-PS-*b*-PMA-*b*-P*t*BA) was synthesized from a norbornene-functionalized chain transfer agent (NB-CTA) by sequential RAFT polymerizations. Placement of the polymerizable norbornenyl unit at the polystyrene chain terminus was done so that its polymerization into a molecular brush would present the hydrophobic materials within the inner region of the final supramolecularly assembled structures, after converting the *tert*-butyl acrylate portion of the polyacrylate chain segments to poly(acrylic acid). However, the reinitiation of polymerization is usually disfavored when growing polyacrylates from polystyrene macroCTAs. Another challenge in this step is the participation of norbornenyl groups in the multiple radical polymerizations, which would destroy the defined macromolecular architecture and prevent later conversion into the molecular brush topology. Therefore, the polymerization conditions (temperature, solvent, monomer conversion, and initiator feed ratio) were tuned carefully (see Supporting Information and previous reports[25,28]).

The well-controlled structure of the macromonomer was confirmed by both ^{1}H NMR spectroscopy and gel permeation chromatography (GPC), as shown in Figure 1B. Obvious peak position shifts were observed after each chain extension and the corresponding

Received: October 13, 2010
Published: January 4, 2011

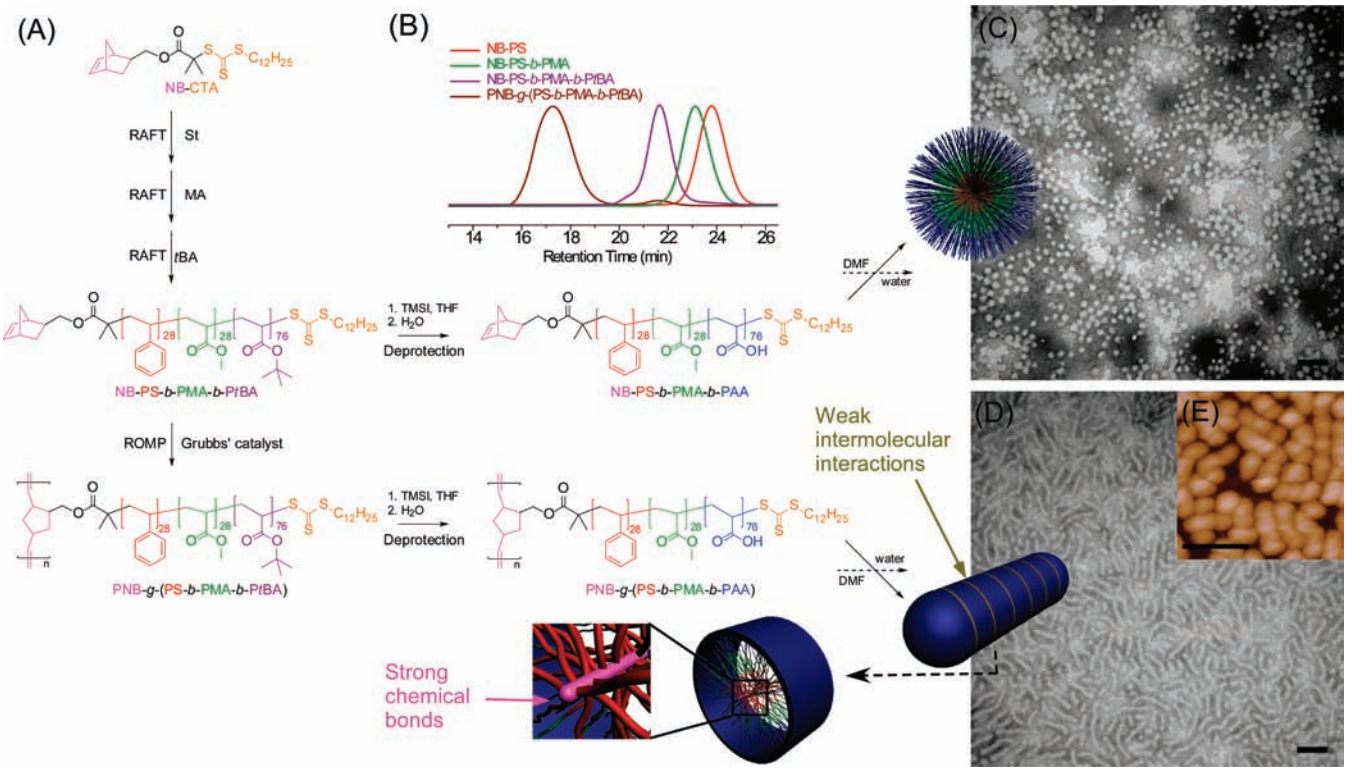

Figure 1. (A) Synthesis and self-assembly of concentrically amphiphilic molecular brushes, having triblock PS-*b*-PMA-*b*-PAA side chains, and linear amphiphilic PS-*b*-PMA-*b*-PAA triblock copolymers. (B) Gel permeation chromatography profiles of NB-PS, NB-PS-*b*-PMA, NB-PS-*b*-PMA-*b*-P*t*BA, and PNB-*g*-(PS-*b*-PMA-*b*-P*t*BA). (C) TEM image of the nanostructures self-assembled from linear NB-PS-*b*-PMA-*b*-PAA triblock copolymers in solution and then cast onto a carbon-coated copper grid. (D) TEM image of the hierarchical cylindrical nanostructures comprised of PNB-*g*-(PS-*b*-PMA-*b*-PAA) self-assembled in solution and then cast onto a carbon-coated copper grid. (E) AFM image of the hierarchical cylindrical nanostructures comprised of PNB-*g*-(PS-*b*-PMA-*b*-PAA) self-assembled in solution and then cast onto a mica substrate. Scale bar: 100 nm.

peaks were all symmetric, indicating monomodal molecular weight distributions with low polydispersity indices (PDIs). The final macromonomer (NB-PS-*b*-PMA-*b*-P*t*BA) had a molecular weight of 15 900 Da with a PDI of 1.20.

The backbone of the overall molecular brush (PNB-*g*-(PS-*b*-PMA-*b*-P*t*BA)) was grown in the second step, by ROMP of the chain end norbornenyl groups of NB-PS-*b*-PMA-*b*-P*t*BA. ROMP has been widely used to polymerize bulky macromonomers to afford densely grafted polymers.[25−28,31−34] As shown in the GPC trace (Figure 1B), a peak shift to a lower retention time was observed with over 95% conversion of the macromonomers to brush structures. The peak at 21−22 min indicates <5% of residual macromonomer, which is believed to lack a polymerizable norbornenyl chain end,[25,28] due to the mechanism of RAFT polymerization. The resulting molecular brushes had a molecular weight of 1.52×10^6 Da with a narrow molecular weight distribution (PDI = 1.15), which, by the nature of the "grafting-through" procedure, had an even grafting density of side chains along the backbone. Finally, PNB-*g*-(PS-*b*-PMA-*b*-P*t*BA) was then converted to the concentrically amphiphilic block brush copolymer PNB-*g*-(PS-*b*-PMA-*b*-PAA) by deprotection of the acrylic acid groups by acidolysis of the *tert*-butyl acrylate repeat units.

In addition to providing control over the molecular brush structure and composition, the "grafting-through" strategy also offered the opportunity to isolate exact structural and compositional analogs of the linear triblock copolymer side chains. By deprotecting the acrylic acid repeat units of NB-PS-*b*-PMA-*b*-P*t*BA, NB-PS-*b*-PMA-*b*-PAA was obtained, whose composition is consistent with the side chains of the molecular brush. The solution-state assembly behaviors of these two amphiphilic macromolecules—one being a complex molecular brush architecture and the other being a linear polymer chain—were then investigated and compared.

When transitioned from *N*,*N*-dimethylformamide into water, the nanostructures from the triblock molecular brush copolymer and linear copolymer amphiphiles exhibited different morphologies, regardless of their compositional consistency. As shown in the transmission electron microscopy (TEM) images, the linear amphiphilic macromolecules gave globular nanoscopic morphologies with overall diameters of 21 ± 2 nm (Figure 1C), while the molecular brushes exhibited cylindrical morphologies with diameters of 18 ± 2 nm and lengths of 92 ± 21 nm (Figure 1D). The diameter of the cylinders was close to the diameter of the globules, suggesting that the core−shell micellar arrangement of PS-*b*-PMA-*b*-PAA polymer side chains in the molecular brushes was similar to that of those polymers, not connected by covalent bonds. Under imaging by atomic force microscopy (AFM), it is obvious that the cylindrical nanoassemblies were composed of individual globular structures, presumably individual molecular brushes, arranged by a one-dimensional assembly (Figure 1E and Figure S1). Assuming that the individual brushes were globular, the average number of brushes per cylinder was around four-to-five.

It was hypothesized that within the molecular brush framework, the rigid polynorbornene backbone limited the conformational freedom of the triblock copolymer grafted side chains,

dx.doi.org/10.1021/ja109191z |*J. Am. Chem. Soc.* 2011, 133, 1228–1231

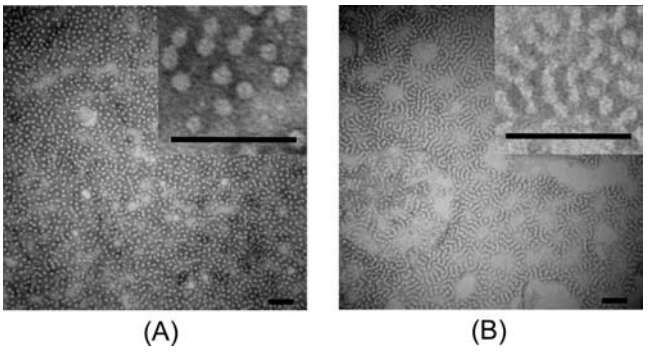

Figure 2. (A) TEM images of the disassembled nanostructures after heating the aqueous solution of PNB-*g*-(PS-*b*-PMA-*b*-PAA) at 70 °C for 3 h. (B) TEM images of the partially reassembled nanostructures after adding an equivalent volume of THF to the heated PNB-*g*-(PS-*b*-PMA-*b*-PAA) aqueous solution. Scale bar: 100 nm.

providing opportunities for interactions unidirectionally between individual molecular brushes, especially by interactions at the backbone chain ends where the density of chains would be minimized. The linear amphiphilic triblock copolymer requires multimolecular interactions to remain as stable dispersions in water. When confined through covalent bonds within the molecular brush architecture, aqueous dispersions of the discrete triblock copolymers would be stabilized by the PAA segments of surrounding chains, but only to a limited extent. Assembly through contacts between the hydrophobic interior (PS and PMA) counterparts from multiple molecular brushes would reduce the intrinsic energy and, thereby, retain their multimolecular assembly tendency. By having lower density, less well stabilized and active end caps on the molecular brushes, one-dimensional assembly would be promoted, to afford the cylindrical nanostructures as observed.

To further study this proposed mechanism, the aqueous solution was heated at 70 °C for 3 h. Upon heating, it was found that the cylindrical morphologies were replaced by globular entities with a number-averaged diameter of 19 ± 2 nm, as observed by TEM, suggesting that disassembly of the cylindrical nanostructures into individual brushes had occurred (Figure 2A). The disassembly was further confirmed by dynamic light scattering (DLS) analysis of the PNB-*g*-(PS-*b*-PMA-*b*-PAA) aqueous solutions at different temperatures, which showed that the hydrodynamic sizes of the nanostructures decreased when the temperature was increased from 25 to 70 °C (Figure S3). The disassembly can be explained by analyzing the forces in the cylindrical structures to bring the triblock copolymer chains together. There were two interactions involved in the cylindrical nanostructures: One was the strong covalent bonds which held the amphiphilic triblock copolymer onto the polynorbornene backbone; the other was the weak intermolecular noncovalent interactions that assembled individual brushes into cylindrical structures. Heating the solution provided sufficient energy to break the weak intermolecular interactions, but the strong covalent bonds were still conserved by this process. The disassembly confirmed that the cylindrical nanostructures resulted from the self-assembly of the amphiphilic molecular brushes *via* intermolecular interactions.

Interestingly, cooling the heated solution at room temperature could not reproduce the cylindrical structures, even after concentrating the solution 10-fold to increase the frequency of intermolecular collisions between molecular brushes. This result suggested that the interaction between the hydrophobic core domains of amphiphilic molecular brushes is a key parameter to their self-organization behaviors. After being disassembled by heat, the individual brushes had to adopt conformations in which the inner hydrophobic cores were fully surrounded by hydrophilic shells to decrease the intrinsic energy. As a result, the cores became inaccessible, leading to an incapability to interact with each other to reproduce the cylindrical nanostructure.

Changing the environmental medium can change the conformations, conformational degrees of freedom, mobility, and dynamics of individual brushes. An equivalent volume of THF was added to the heated micellar solution, from which TEM images showed that cylindrical nanostructures appeared, suggesting that the hydrophobic domains became accessible and interactive again after adding a common solvent, which led to attraction between individual molecular brushes (Figure 2B). Furthermore, the heated solution was lyophilized, and the resulting powders were dissolved in DMF and dialyzed against water again to reproduce the cylindrical structures (Figure S2). The results from TEM showed cylindrical structures with similar sizes to the original assemblies prior to heating. In addition to providing mechanistic insights, the thermally driven disassembly and solvent-promoted reassembly are interesting triggers to alter these unique morphologies.

More insights into the mechanism of the self-assembly of molecular brushes were obtained by comparing the molecular brush structures in organic solvent and after dialysis into water, to determine whether any preassembly occurred prior to the aqueous-promoted assembly process. DLS was used to characterize the samples before and after dialysis in the bulk solution state. At 25 °C, the number-averaged hydrodynamic diameter of the molecular brushes in DMF solution before dialysis was 20 ± 6 nm (Figure S4), while the number-averaged hydrodynamic diameter of the assembled structures after dialysis was 134 ± 38 nm (Figure S3). These data indicate a transformation from individual molecular brushes in organic solvent to multimolecular assemblies in water. Furthermore, TEM was used to observe their morphologies in the dry state, after drop deposition onto a carbon-coated copper grid and drying under ambient conditions (Figures S5 and S6). To avoid the possible side effects of water from the aqueous staining solution, RuO_4 vapor was used. Surprisingly, it was found that the samples dried from DMF solution showed long cylindrical structures that appeared to be branched and interconnected with each other, while those from the aqueous solution contained shorter, discrete cylinders. When dried on the TEM grids, the highly flexible and mobile characteristics of the molecular brushes in DMF promoted interactions between them that were not necessarily unidirectional. As a result, some branching sites were observed, facilitated by more than two contact points between one molecular brush and its neighbors. Although the images of Figure S5 are essentially drying patterns, they provide significant information regarding the intermolecular interactions and degrees of flexibility that are possible even for these densely grafted triblock molecular brush copolymers. In comparison, the dynamically assembled structures were "frozen" in water after dialysis, as suggested by both DLS and TEM.

Given the observation that the molecular brushes were discrete, individual entities in DMF solution before dialysis, combined with the fact that the separated individual molecular brushes alone could not undergo intermolecular interactions in water, the self-assembled structures were proposed to be created during dialysis, when the flexibilities of the triblock side chains

dx.doi.org/10.1021/ja109191z |*J. Am. Chem. Soc.* 2011, 133, 1228–1231

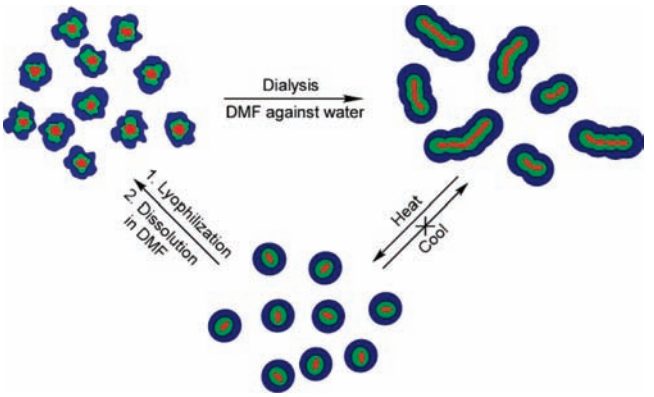

Figure 3. Schematic illustrations of the morphologies of the PNB-*g*-(PS-*b*-PMA-*b*-PAA) molecular brushes at different stages.

were still in an appropriate range for intermolecular interactions and the mobilities of the molecular brushes were decreased significantly to avoid separation of the assembled structures. Overall, a mechanism of the self-assembly of PNB-*g*-(PS-*b*-PMA-*b*-PAA) into dynamic hierarchical cylindrical nanostructures was proposed, as shown in Figure 3.

The hierarchical process demonstrated here, which is developed from applying covalent and supramolecular interactions stepwise to amphiphilic linear triblock copolymers, has enabled the production of dynamic, one-dimensional, cylindrical assemblies. Although originating from a symmetrical, concentrically arranged molecular brush block copolymer structure, the relative chain densities along the primary molecular brush backbone provided for differentiation of accessibility to the core chain segments, greater at the backbone ends than the midsegment, to produce these complex hierarchically assembled nanomaterials. With all of the attention that is being placed upon the incorporation of chemically distinct functionalities within polymer frameworks, this physically induced asymmetry is an exciting new direction to take as a general methodology toward the preparation of other unique materials. In fact, the combination of recent advances in synthetic polymer chemistry and solution-state assembly can be tuned individually, to influence their intra- and intermolecular interactions, and facilitate the arrangement of polymer building blocks into complex, functional materials, ultimately, approaching the sophistication of Nature.

■ ASSOCIATED CONTENT

Supporting Information. Detailed experimental section, TEM images, AFM images, DLS histograms, and ref 10 full author listing. This material is free of charge via the Internet at http://pubs.acs.org.

■ AUTHOR INFORMATION

Corresponding Author
wooley@chem.tamu.edu

■ ACKNOWLEDGMENT

This research is supported by the National Science Foundation (Grant Numbers DMR-0906815 and DMR-1032267) and by fellowship support from the McDonnell International Scholars Academy (to Z.L.) The Welch Foundation is gratefully acknowledged for partial support through the W. T. Doherty-Welch Chair in Chemistry, Grant No. A-0001. We also thank the electron microscopy facilities at Washington University in St. Louis, Department of Otolaryngology, Research Center for Auditory and Visual Studies funded by NIH P30 DC004665.

■ REFERENCES

(1) Whitesides, G. M.; Grzybowski, B. *Science* **2002**, *295*, 2418–2421.
(2) Dobson, C. M. *Nature* **2003**, *426*, 884–890.
(3) Zhang, S. G. *Nat. Nanotechnol.* **2006**, *1*, 169–170.
(4) Pochan, D. J.; Chen, Z. Y.; Cui, H. G.; Hales, K.; Qi, K.; Wooley, K. L. *Science* **2004**, *306*, 94–97.
(5) Zhang, L. F.; Eisenberg, A. *Science* **1995**, *268*, 1728–1731.
(6) Zubarev, E. R.; Pralle, M. U.; Sone, E. D.; Stupp, S. I. *J. Am. Chem. Soc.* **2001**, *123*, 4105–4106.
(7) Mirkin, C. A.; Letsinger, R. L.; Mucic, R. C.; Storhoff, J. J. *Nature* **1996**, *382*, 607–609.
(8) Li, Z. B.; Kesselman, E.; Talmon, Y.; Hillmyer, M. A.; Lodge, T. P. *Science* **2004**, *306*, 98–101.
(9) Rothemund, P. W. K. *Nature* **2006**, *440*, 297–302.
(10) Percec, V.; et al. *Science* **2010**, *328*, 1009–1014.
(11) Wang, X. S.; Guerin, G.; Wang, H.; Wang, Y. S.; Manners, I.; Winnik, M. A. *Science* **2007**, *317*, 644–647.
(12) Walther, A.; Drechsler, M.; Rosenfeldt, S.; Harnau, L.; Ballauff, M.; Abetz, V.; Müller, A. H. E. *J. Am. Chem. Soc.* **2009**, *131*, 4720–4728.
(13) Dupont, J.; Liu, G. J.; Niihara, K.; Kimoto, R.; Jinnai, H. *Angew. Chem., Int. Ed.* **2009**, *48*, 6144–6147.
(14) Yin, P.; Choi, H. M. T.; Calvert, C. R.; Pierce, N. A. *Nature* **2008**, *451*, 318–U4.
(15) Zhu, X. M.; Beginn, U.; Möller, M.; Gearba, R. I.; Anokhin, D. V.; Ivanov, D. A. *J. Am. Chem. Soc.* **2006**, *128*, 16928–16937.
(16) Ikkala, O.; ten Brinke, G. *Science* **2002**, *295*, 2407–2409.
(17) Böker, A.; Lin, Y.; Chiapperini, K.; Horowitz, R.; Thompson, M.; Carreon, V.; Xu, T.; Abetz, C.; Skaff, H.; Dinsmore, A. D.; Emrick, T.; Russell, T. P. *Nat. Mater.* **2004**, *3*, 302–306.
(18) Jones, R. *Nat. Nanotechnol.* **2008**, *3*, 699–700.
(19) Sheiko, S. S.; Sumerlin, B. S.; Matyjaszewski, K. *Prog. Polym. Sci.* **2008**, *33*, 759–785.
(20) Zhang, M. F.; Müller, A. H. E. *J. Polym. Sci., Part A: Polym. Chem.* **2005**, *43*, 3461–3481.
(21) Börner, H. G.; Beers, K.; Matyjaszewski, K.; Sheiko, S. S.; Möller, M. *Macromolecules* **2001**, *34*, 4375–4383.
(22) Cheng, C.; Qi, K.; Khoshdel, E.; Wooley, K. L. *J. Am. Chem. Soc.* **2006**, *128*, 6808–6809.
(23) Zhang, M. F.; Breiner, T.; Mori, H.; Müller, A. H. E. *Polymer* **2003**, *44*, 1449–1458.
(24) Gao, H. F.; Matyjaszewski, K. *J. Am. Chem. Soc.* **2007**, *129*, 6633–6639.
(25) Li, Z.; Ma, J.; Cheng, C.; Zhang, K.; Wooley, K. L. *Macromolecules* **2010**, *43*, 1182–1184.
(26) Xia, Y.; Kornfield, J. A.; Grubbs, R. H. *Macromolecules* **2009**, *42*, 3761–3766.
(27) Xia, Y.; Olsen, B. D.; Kornfield, J. A.; Grubbs, R. H. *J. Am. Chem. Soc.* **2009**, *131*, 18525–18532.
(28) Li, Z.; Zhang, K.; Ma, J.; Cheng, C.; Wooley, K. L. *J. Polym. Sci., Part A: Polym. Chem.* **2009**, *47*, 5557–5563.
(29) Bielawski, C. W.; Grubbs, R. H. *Prog. Polym. Sci.* **2007**, *32*, 1–29.
(30) Moad, G.; Rizzardo, E.; Thang, S. H. *Aust. J. Chem.* **2005**, *58*, 379–410.
(31) Nyström, A.; Malkoch, M.; Furó, I.; Nyström, D.; Unal, K.; Antoni, P.; Vamvounis, G.; Hawker, C. J.; Wooley, K.; Malmström, E.; Hult, A. *Macromolecules* **2006**, *39*, 7241–7249.
(32) Buchowicz, W.; Holerca, M. N.; Percec, V. *Macromolecules* **2001**, *34*, 3842–3848.
(33) Percec, V.; Schlueter, D. *Macromolecules* **1997**, *30*, 5783–5790.
(34) Cheng, C.; Yang, N. L. *Macromolecules* **2010**, *43*, 3153–3155.